Gas Permeance Measurement of Hollow Fiber Membranes in Gas-Liquid Environment

Laura W. Lund
McGowan Institute for Regenerative Medicine, Dept. of Bioengineering

Brack G. Hattler
McGowan Institute for Regenerative Medicine, Dept. of Surgery

William J. Federspiel
McGowan Institute for Regenerative Medicine,
Dept. of Chemical Engineering, Dept. of Surgery, and Dept. of Bioengineering

University of Pittsburgh, Pittsburgh, PA 15219

An apparatus and methodology were developed to measure the oxygen and carbon dioxide permeance of hollow fiber membranes (HFMs) in a gas-liquid environment. The gas-liquid permeance measurements were compared with measurements made in a gas-gas environment to validate the methodology and to determine whether the permeance of an HFM in a gas-liquid environment differs inherently than in a gas-gas environment. The methodology is based on measuring the overall system permeance for a range of liquid velocities and isolating the membrane resistance to gas flux from the liquid boundary layer resistance by regression of a nonlinear system model to the data. The success of the methodology in accurately estimating membrane permeance depended on the maximum liquid velocity which the system could consistently generate past the fibers.

Introduction

In certain applications of HFM gas exchange modules, the permeance of the membrane wall must be evaluated while exposed to a liquid environment on one side. In bioengineering, examples of such applications are the permeance of biohybrid fibers for next generation artificial lung devices (Ohata et al., 1998), or the effect of thrombus formation on permeance of the fibers of blood oxygenation devices. Indeed, this article describes a methodology developed to evaluate the permeance of hydrophobic hollow fiber membranes in a gas-liquid environment for the selection of an optimal fiber for an intravenous extended term blood oxygenation device. This methodology would not only be of utility to blood oxygenation, however, but also of utility within the general field of membrane separations.

Measurement of the gas permeance of HFMs in a gas-liquid environment requires a method for isolating the serial resistances of the liquid concentration boundary layer from that of the membrane wall. A gas-liquid permeance measurement apparatus was developed which requires a minimal volume of liquid, can be quickly and inexpensively manifolded with any fiber sample of interest, requires only gas-side concentration measurements to estimate the overall system permeance, and can be used with any liquid of interest, including blood. The methodology is based on measuring the overall system permeance for a range of liquid velocities and isolating the membrane resistance to gas flux from the liquid boundary layer resistance by regression of a nonlinear system model to the data. The HFM permeances estimated using this apparatus and methodology were compared with measurements made in a gas-gas environment to validate the methodology and to confirm that the permeance of a HFM in a gas liquid environment is not effectively different than in a gas-gas environment.

There are very few reports of the use of a methodology for measuring the permeance of HFMs in a gas-liquid environment, and in each of the few cited cases there have been unresolved issues identified by the results. Yasuda and Lamaze (1972) studied the gas permeance of microporous and nonporous membrane sheets in a gas-liquid system by mixing the liquid phase, but were unable to fully remove the effects of the liquid boundary layer from the membrane permeance measurements. Both Keller and Shultis (1979) and Qi and

Correspondence concerning this article should be addressed to L. W. Lund.

Cussler (1985) recognized that fiber membrane permeance measurements in a gas-liquid system are affected by small diffusional boundary layers which exist in the liquid side subjacent to the fibers, even in the presence of substantial bulk liquid mixing. Keller and Shultis attempted to measure oxygen permeance of both microporous and true membrane fibers in a gas-liquid environment by using a liquid which rapidly reacted with oxygen and in theory eliminated the liquid concentration boundary layer and thus the liquid-phase resistance to oxygen flux. However, they found that the permeance of the microporous membranes was as low as that of the nonporous true membranes, which they suggested was due to water penetration into the pores. Similarly, Qi and Cussler measured the CO_2 permeance of microporous HFMs in a gas-liquid system by using a liquid which rapidly reacted with CO_2 to eliminate the liquid-phase resistance, but also found the microporous membrane permeance to be several orders of magnitude less than expected. Their study concluded that, even for hydrophobic fibers, microporous membrane permeance lies intermediate between the limits of gas-filled and liquid-filled pores.

The results from both studies indicate either that the methodology used was not effective in eliminating the liquid-phase resistance to gas flux, or that the permeance of a hydrophobic microporous membrane in a gas-liquid environment is inherently lower than it would be in a gas-gas environment (assuming no convective flux). Either conclusion suggests that the development and validation of a method for measuring HFM permeance in a gas-liquid environment is important. The method used by Keller and Shultis, as well as Qi and Cussler, did not definitively show that the liquid-phase resistance was eliminated, and, furthermore, does not lend itself to the study of HFMs in different liquids, such as plasma or blood. Yet, if their hydrophobic microporous membrane permeance measurements were in fact valid, then a study of the mechanisms responsible for the difference between gas-liquid and gas-gas permeance is warranted because of its large potential effect on the overall gas exchange performance of a HFM gas exchange module.

Initial permeance measurements made using this methodology were previously reported for microporous HFMs in water at 37°C (Lund et al., 1996). The estimates of membrane permeance from these measurements were two orders of magnitude lower than calculated estimates of microporous HFM permeance. The unexpectedly low estimates of membrane permeance were attributed to liquid infiltration of the pores, as was suggested by Keller and Shultis (1979) and Qi and Cussler (1985). However, the desire to more definitively validate this conclusion drove a progression of improvements to the apparatus and methodology. In subsequent tests of HFMs having a large range of permeances, and by comparison of gas-liquid results with gas-gas measurements and scrutiny of the nonlinear regression procedure used to estimate permeance of the fibers in a gas-liquid environment, this research effectively demonstrates that the use of the gas-liquid methodology is effective only within a limited range of membrane permeance determined by the level of mixing in the liquid phase of the test apparatus.

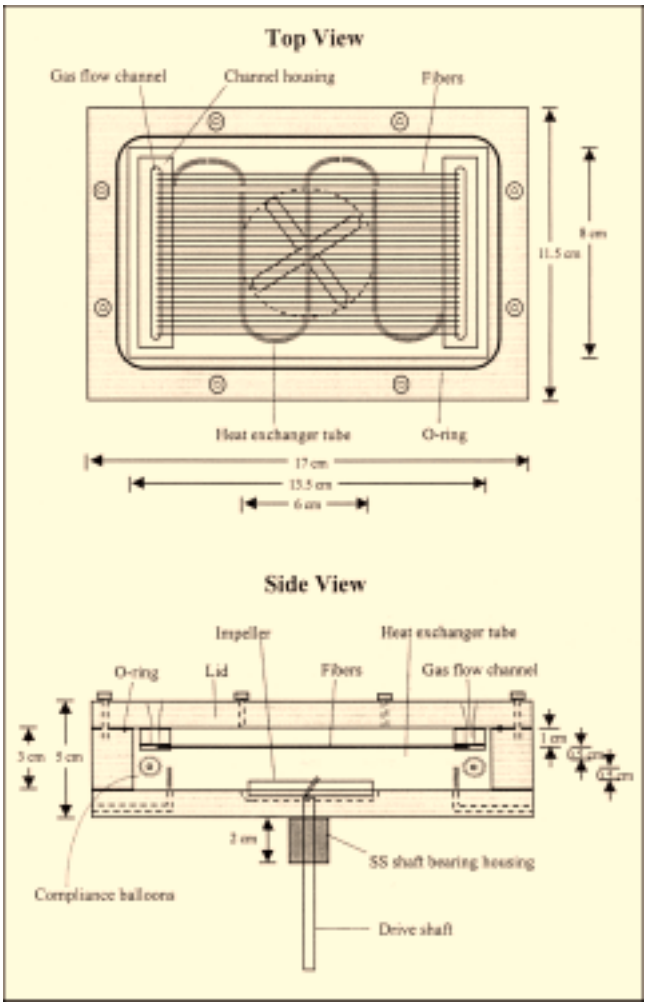

Figure 1. Diffusion chamber.

Apparatus

The central component of the measurement procedure is a diffusion chamber, which consists of a parallel arrangement of the HFMs submerged in a closed, stirred liquid bath of fixed volume. This apparatus was specifically designed for the gas permeance measurement of membranes having a hollow fiber configuration functioning in a gas-liquid environment where the gas phase flows through the fiber lumen and the liquid phase is in contact with the the outside of the fiber wall. The diffusion chamber design is shown in Figure 1. Approximately 100 fibers of 10 cm in length are manifolded in a parallel arrangement to gas flow channels extending from interchangeable lids mounted to the diffusion chamber with screws and sealed with a large o-ring. The interior of the chamber is fitted with a stainless steel heat exchange tube for temperature regulation of the liquid in the chamber. The diffusion chamber is also equipped with a small interior compliance balloon to accommodate small changes in liquid volume, and sealed ports for temperature sensing, sample withdrawal, and attachment of a small exterior liquid reservoir bag (for replacement of water vapor flux across the fiber walls). The liquid is stirred by a quadruple pitched blade impeller. The rotating shaft of the impeller passes through a

stainless steel bearing housing which incorporates a dynamic oil seal.

The equipment utilized in conjunction with the diffusion chamber for permeance measurements is shown in Figure 2. The diffusion chamber is mounted to the front plate of a DC motor to drive the impeller. Spin rate of the impeller is measured with a Hall-effect sensor and tachometer fixed to the motor approximately 5 mm above a small magnet mounted to the shaft.

For a given liquid stir rate, the gas permeance of the system is determined from the rate of test gas washout from within the bulk liquid to the gas flow through the fiber lumens. Gas flow through the fibers is driven by a vacuum pump so that pressures within the fibers will not exceed liquid side pressures and potentially result in bubbling of gas through membrane micropores into the liquid. The percent of test gas in the gas flow exiting the fibers is sampled with a mass spectrometer (Model 1100 Medical Gas Analyzer, Marquette Electronics, Jupiter, FL), which provides a voltage output for each gas which the spectrometer is fitted to measure.

Measurement of System Gas Permeance

Washout of a test gas from the well-stirred liquid of fixed volume into the fibers can be described by a mass balance of the test gas within the liquid phase with the following equation

$$\sigma V \frac{dP_\lambda}{dt} = -KA\left[P_\lambda(t) - \bar{P}_g(t)\right] \tag{1}$$

where P_λ is the partial pressure of the test gas in the liquid and is directly proportional to concentration $C_\lambda = \sigma P_\lambda$ (Henry's law), σ is the Henry's law solubility coefficient which is assumed constant for a given liquid temperature, V is the volume of the liquid in the chamber, A is the surface area of the fibers exposed to the liquid, $\bar{P}_g$ is the average partial pressure of the test gas in the gas phase flowing through the fiber lumens, and K is the overall permeance to the test gas of the fiber wall and liquid concentration boundary layer. The solutions to Eq. 1 are of the form

$$P_\lambda(t) = P_\lambda^0 e^{-(t/\tau)} \quad \text{and} \quad \bar{P}_g(t) = \bar{P}_g^0 e^{-(t/\tau)} \tag{2}$$

where P_λ^0 is the partial pressure of the test gas in the liquid at time $t = 0$, $\bar{P}_g^0$ is the average partial pressure of the test gas in the fibers at $t = 0$, and τ is the time constant of the washout. Substitution of the solutions (Eq. 2) into the mass balance Eq. 1 yields the following equation

$$\lambda = \frac{1}{\tau} = \frac{KA}{\sigma V}\left(1 - \frac{\bar{P}_g^0}{P_\lambda^0}\right) \tag{3}$$

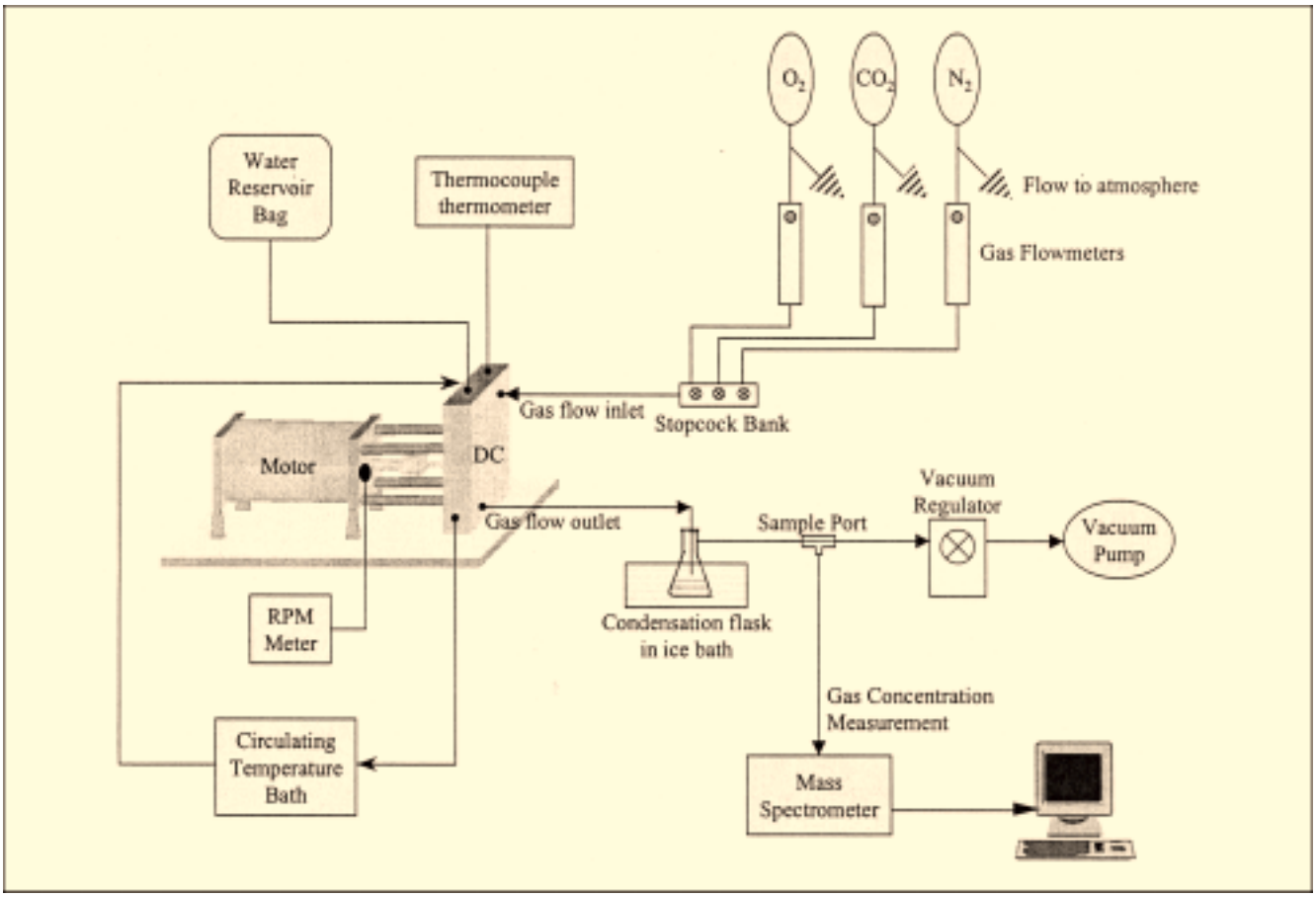

Figure 2. Diffusion chamber apparatus and system equipment used to measure permeance.

where λ is the washout rate constant. If the flow rate of flush gas through the fibers is sufficiently high, then the average partial pressure of the test gas within the fibers will remain appreciably below that within the liquid, and $\bar{P}_g^0/P_\lambda^0 \ll 1$. Under these conditions, the washout rate constant λ is directly proportional to the system permeance and, most conveniently, is independent of the gas-flow rate through the fibers. The system permeance K can therefore be calculated from the measured washout decay rate and known system parameters using the equation

$$K = \lambda \frac{\sigma V}{A} \tag{4}$$

The assumption leading to Eq. 4 was validated by measuring the decay rate at a specified temperature and impeller stir rate using a series of gas flows to demonstrate a consistent permeance K.

To perform the system permeance measurement, the liquid is stirred at a set rate and is first equilibrated with 100% of the test gas drawn under vacuum through the fibers. The fiber gas source is then switched to an alternate gas source so that the concentration of test gas entering the fibers is 0%. The concentration of the test gas exiting the fibers is continuously measured using the mass spectrometer and is recorded to a personal computer. The rate of the exponential washout of the test gas from the liquid can then be determined by regression of a single exponential decay equation to the recorded data, and used to calculate the effective permeance K of the fiber-liquid system. These measurements are repeated for an array of stir rates between 100 and 1,200 rpms.

Estimation of Membrane Permeance

In a gas-liquid environment, the overall system permeance K to the test gas is simply the reciprocal of the overall resistance to the transfer of gas from the liquid to the gas phase within the fiber lumen. Assuming negligible resistance to gas transfer in the gas phase within the fiber lumen, the overall resistance is governed by the serial resistances of the membrane wall R_m and the concentration boundary layer R_λ, which forms in the blood phase on the exterior surface of the fibers, that is

$$R_T = R_m + R_\lambda \quad \text{or} \quad \frac{1}{K} = \frac{1}{K_m} + \frac{1}{K_\lambda} \tag{5}$$

where K_m is the permeance of the HFM and K_λ is the mass-transfer coefficient of the liquid concentration boundary layer. By dimensional analysis, the liquid boundary layer mass-transfer coefficient can be represented by an empirical Sherwood correlation $Sh = cRe^{\beta}Sc^{1/3}$, where Sh is the Sherwood number, Re is the Reynolds number, Sc is the Schmidt number, c is a correlation constant, and β is the correlation exponent. Based on this correlation, the dependence of K_λ on the system parameters can be reduced to the form $K_\lambda = \alpha\Omega^{\beta}$, where α is a lumped constant representing all constant parameters which do not vary as a function of liquid velocity (that is, fiber diameter, impeller diameter, kinematic viscosity of fluid, and diffusivity and solubility of test gas in liquid), and Ω is the impeller stir rate representing liquid velocity. Equation 5 can thus be rewritten as

$$K = \left(\frac{1}{K_m} + \frac{1}{\alpha\Omega^{\beta}} \right)^{-1} \tag{6}$$

Equation 6 serves as a nonlinear model of the overall system permeance K as a function of the liquid stir rate. By regression of the model equation to measurements of K vs. Ω, the three model parameters (K_m, α, and β) can be estimated. Because the degree of nonlinearity of a model equation affects how the model performs, nonlinear regression was also conducted using an alternative form of the model Eq. 6 given as

$$\text{Form 2:} \quad R = R_m + \gamma\Omega^{-\beta} \tag{7}$$

where $R = 1/K$ which is calculated from K prior to performing the regression, $R_m = 1/K_m$, and $\gamma = 1/\alpha$. Thus, for Form 2 of the model, the estimated parameters are R_m, γ, and β.

Nonlinear regression of the model to the data was accomplished by using the method of least squares to determine the set of parameters. The standard errors of the model parameter estimates were found from the diagonal elements of the covariance matrix approximated using nonlinear parameter estimation theory (Beck and Arnold, 1977; Lutchen et al., 1988).

Fibers Tested

The hollow fiber membranes (HFMs) tested within the scope of this research were either commercially available fibers, or were proprietary fibers manufactured for specific applications graciously provided to us as samples for our research. Both microporous and composite HFMs were tested. The microporous fibers tested were made from hydrophobic polypropylene so their pores would remain gas filled in an aqueous gas-liquid environment. All composite fibers were manufactured to have an ultrathin nonporous polymer layer at the exterior fiber surface of a microporous wall. However, complete pore coverage was not an essential constraint. The composite fibers were chosen such that a full range of permeances could be evaluated to effectively characterize the gas-liquid permeance measurement methodology.

The microporous fibers were Celgard X30-240 (Celgard LLC, Charlotte, NC), which had an outer diameter of 300 μm, an inner diameter of 240 μm, and a pore width of 0.030 μm. Four composite, or coated, hollow fiber membranes were tested with each coated with a different polymer associated with patented or proprietary coating processes. The first were high permeance fibers consisting of Celgard X30-240 fibers coated with a patented process (Nemser and Roman, 1991) by Compact Membrane Systems. The second and third were medium range permeance composite fibers provided by Dainippon Ink and Chemical (DIC, Tokyo, Japan), and Senko Medical Instruments Manufacturing Company (Tokyo, Japan). The DIC fibers had an outer and inner diameter of 255 and 205 microns, respectively. The Senko fibers were

coated using Celgard X30-240 fibers and a plasma polymerization process developed and patented by Surface Engineering Technologies (SET, Salt Lake City UT) (Hu et al., 1995). The fourth composite fiber was provided by Bend Research and was coated by special request to have a lower range permeance using Celgard X30-240 fibers and a proprietary dip coating process in the early stages of development. Note that these fibers were obtained not for their material properties, but rather for their levels of permeance and nonporous coated nature which were relevant to long-term blood oxygenation. Although complete coating was desirable, permeance was of utmost importance which meant that some of the composite fibers tested were not 100% defect free.

Gas-gas permeance measurements of both microporous and coated HFMs were measured to validate the methodology for estimation of HFM permeance in a gas-liquid environment. In a gas-gas environment, the resistances to gas flux in the gas phases on either side of the membrane wall are negligible compared to the resistance of the wall itself and thus the permeance of the membrane wall can be measured directly. Based on the average pore width of the Celgard X30-240 microporous fibers of 0.03 μm, the Knudsen number falls between 10–20 for carbon dioxide, oxygen and nitrogen for temperatures between 23 and 37°C. For Knudsen numbers between the range of 10–100, flow within the pores can be described by the Knudsen diffusion equation to within 10% (Brodkey and Hershey, 1988). Therefore, for the microporous fibers tested, gas flux across the membrane wall in a gas-gas environment should be independent of the absolute pressure difference, and thus the mechanism for gas flux through the pores will be the same as in a gas-liquid environment.

Three methods were used to measure the gas-gas permeance of the hollow fiber membranes where possible. Multiple methods were used to validate their results because of the lack of permeance information available for these fibers due to the proprietary nature of the coating process or the modification of their coating to suit our needs. Two of the gas-gas permeance measurements methods were performed on the very same fiber lids used to measure permeance in the gas-liquid test system. For the first method, the fibers were bathed on the exterior with the test gas of interest (O_2 or CO_2), and nitrogen was swept through the fiber lumen. The fiber permeance was determined using an equation derived from a mass balance of the test gas within the fiber lumen where the difference in the mass flow of test gas entering and exiting the fiber is equal to the flux of test gas across the membrane wall

$$K_m = \frac{(\%G)_L \dot{m}_L}{\left(pG_{\text{out}} - \overline{pG}_{\text{in}}\right) A} \tag{8}$$

where $(\%G)_L$ was the percent of test gas exiting the fibers measured with a mass spectrometer, $\dot{m}_L$ was the mass-flow rate measured at the exit of the fiber bank, pG_{out} was the partial pressure of the test gas outside of the fibers (equal to total pressure since 100% test gas), and $\overline{pG}_{\text{in}}$ is the average partial pressure of the test gas within the fibers determined from an average of the total pressure at the entrance and exit of the fibers multiplied by half the percent test gas at the exit, and A was the total exterior fiber surface area.

The second method for measuring the fiber permeance in a gas-gas environment was performed by fastening the lid of fibers to the diffusion chamber and sealing the entrance to the gas-flow path through the fibers. The outside fiber surfaces were thus enclosed within the diffusion chamber, which was pressurized with 100% test gas. The partial pressure gradient across the membrane wall drove flux of the test gas from outside of the fibers into the lumens and out the open exit pathway. The flow rate of test gas out of the fibers was measured with a bubble flow meter and used directly to calculate membrane permeance with the following equation

$$K_m = \frac{\dot{m}_L}{(P_{\text{out}} - P_L) A} \tag{9}$$

where $\dot{m}_L$ is the mass-flow rate rate exiting the fibers (mL^{STP}/s), P_{out} and P_L are the absolute pressures outside the fibers and at the exit to the fiber lumens, respectively, and A is the membrane surface area based on the nominal outer diameter of the fibers. Because the percent of test gas is 100% on both sides of the fiber wall, partial pressure is simply the absolute pressure and thus measurement of test gas concentration is not necessary. The pressure drops along the lumen of the fibers for this system were negligible (less than 5 mm Hg). Therefore, the total pressure at the exit of the fibers P_L was used to represent the average partial pressure within the

Table 1. Gas-Gas Permeance Measurements

Fiber			Bend	DIC	Senko	CMS*	Celgard X30-240*
Membrane Permeance ($ml^{STP}/s \cdot cm^2 \cdot cm\ Hg$)	CO_2	Method 1	5.30×10^{-5}	2.73×10^{-4}	4.60×10^{-4}	N/A	N/A
		Method 2	4.36×10^{-5}	2.09×10^{-4}	4.23×10^{-4}	4.25×10^{-3}	1.47×10^{-2}
		Method 3	5.01×10^{-5}	2.62×10^{-4}	4.20×10^{-4}	N/A	N/A
	O_2	Method 1	1.24×10^{-5}	2.78×10^{-4}	1.72×10^{-4}	N/A	N/A
		Method 2	1.09×10^{-5}	1.84×10^{-4}	1.67×10^{-4}	2.25×10^{-3}	1.72×10^{-2}
		Method 3	1.48×10^{-5}	2.78×10^{-4}	1.56×10^{-4}	N/A	N/A
Selectivity	CO_2/O_2	Method 1	4.3	1.0	2.7	N/A	N/A
		Method 2	4.0	1.1	2.5	1.9	0.9
		Method 3	3.4	0.9	2.7	N/A	N/A

*For high permeance fibers, use of Method 1 was not effective, because the high percent test gas at fiber exit resulted in gas-flow limited exchange. For Method 3, CMS fibers were no longer available for testing.

fibers to determine the partial pressure gradient across the membrane wall ($P_{out} - P_L$). This method involved fewer measurements and less equipment than the first and was therefore less prone to error. To verify that there were no leaks in the system, the mass spectrometer was used to confirm that there was no nitrogen in the flow exiting the fibers.

Finally, a third set of measurements were made using essentially the same method as the second, but with a separate smaller sample of fibers from the same original batches. The gas-gas permeance measurement results for all fibers tested are presented in Table 1. For the microporous fibers, the permeance measurements were consistent over a range of absolute pressure differences of 50 to 500 mm Hg (6.7 to 67 kPa), validating Knudsen diffusion through the pores.

Results of Gas-Liquid Permeance Measurements

The results of the gas-liquid permeance measurements are shown in Figure 3. For each data set, a plot of the model equation (smooth line) based on the best-fit parameters from nonlinear regression is also shown for the coated fiber data sets. The resulting estimates of membrane permeance from the gas-liquid measurements using both forms of the system model are shown in Figure 4 in comparison with the direct measurements of membrane permeance made in a gas-gas environment.

The fibers custom coated by Bend had the lowest measured gas-gas permeance, and the estimates of membrane permeance from the gas-liquid system permeance measurements were within 15% of the gas-gas measurements for both oxygen and carbon dioxide with standard errors of less than 12% using both forms of the system model. The gas-gas permeances of the Senko and DIC fibers were approximately an order of magnitude greater than those of the more thickly coated Bend fibers. The membrane permeance for the Senko and DIC fibers using the gas-liquid permeance measurements were consistent with the gas-gas measurements using Form 2 of the model, but were significantly underestimated using Form 1, especially for the oxygen data. The standard errors of the estimates generated using Form 2 were reasonable for the carbon dioxide data, but were larger for the oxygen data, although the value of the estimates were consistent with the gas-gas measurements. The CMS fibers had the highest permeances. For these fibers, nonlinear regression with both forms of the system model resulted in significant underestimation of gas-liquid membrane permeance. Like the CMS fibers, the microporous fiber membrane permeance was significantly underestimated in comparison with the gas-gas measurements by as much as two orders of magnitude. Unique to the microporous fiber data was the dependence of the membrane permeance estimate on the initial guess used to perform the nonlinear regression analysis. The values obtained were thus unreliable and are therefore not listed in the table of membrane permeance estimates.

Discussion

The results show that the gas exchange permeance of HFMs in a gas-liquid system can be estimated by measuring the overall system permeance for a range of liquid flow rates and

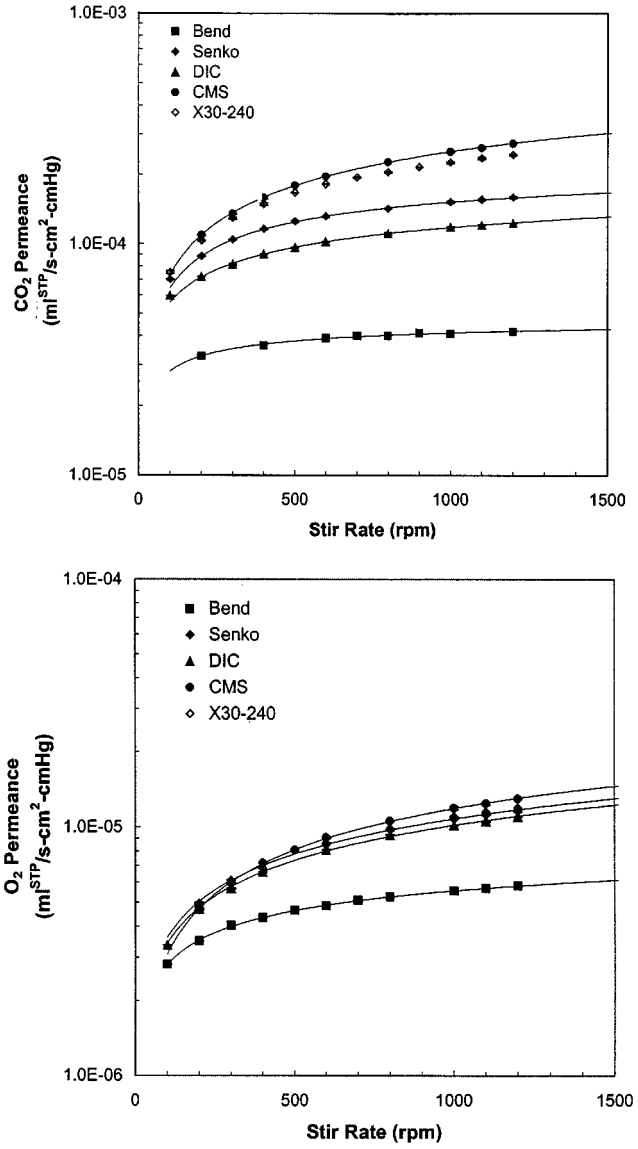

Figure 3. Gas-liquid permeance measurements as a function of the system stir rate.

Resulting regression lines for coated fiber data sets are shown as smooth lines.

using nonlinear regression to isolate the membrane permeance from the liquid boundary layer mass-transfer coefficient, but only for membrane permeances below a certain level. Furthermore, the use of Form 2 of the model yielded better estimates than Form 1 for higher permeance fibers. To understand these results, a more in-depth investigation of the nonlinear regression procedure was conducted.

A sensitivity analysis was performed to measure how responsive both models were to possible values of the three parameters for the rang of the independent variable (stir rate, Ω) over which the data was measured. A more useful means of analyzing sensitivity of a nonlinear model is to compare the *normalized* sensitivity. For each parameter, the normalized sensitivity coefficient $S^n_{\theta_i}$ was calculated as a function of the input, or independent, variable Ω using the following

equation

$$S^n_{\theta_i} = \frac{\theta_i^*}{K}\frac{\partial K}{\partial \theta_i} \tag{10}$$

which represents the percent change in K for a unit percent change in the parameter θ_i (Lutchen and Jackson, 1987). The results of the sensitivity analysis are shown in Figure 5. Three K_m values were chosen for the sensitivity analyses: a high value corresponding to one order of magnitude greater than K_λ at the maximum liquid stir rate (1,200 rpms), a medium value equal to the maximum K_λ, and a low value one order of magnitude less than the maximum K_λ. The upper plots of Figure 5 are the sensitivity analyses for the high K_m situation, the middle plots for the medium K_m, and the lower plots for the low K_m. The solid lines correspond to K_m sensitivity, the dashed lines to a α sensitivity, and the crossed lines to β sensitivity.

For both model forms, the sensitivity to K_m was much lower than to α and β when the value of K_m was an order of magnitude greater than the maximal K_λ. In other words, the parameter estimation technique will have difficulty estimating K_m if it is this high relative to K_λ. However, K_m sensitivity was well balanced with α and β sensitivity when in the medium range, indicating that the regression technique should be able to estimate all three parameters. For low K_m, the K_m sensitivity became very high, but at the cost of sensitivity to α and β. From these plots, it would appear that the regression technique will perform best when the actual K_m falls within a range that is close to or below the maximal K_λ value for the gas-liquid combination being tested, but will still have some sensitivity to high K_m values one order of magnitude greater than the maximal K_λ. Additionally, the sensitivity plots indicated that K_m sensitivity continues to increase for larger stir rates (model independent variable) meaning that data points at the higher stir rates will result in improved K_m sensitivity. In contrast, for α and β with K_m in the medium and low range, the model was more sensitive to data points at low stir rates, from which it was concluded that a range of data points fully spanning the drive capacity of the motor and tachometer would result in the most effective regression results.

From the consistency of the gas-liquid membrane permeance estimates of the Bend, Senko, and DIC fibers with the gas-gas measurements using Form 2 of the model, it was concluded that the permeance of a coated HFM in a gas-liquid

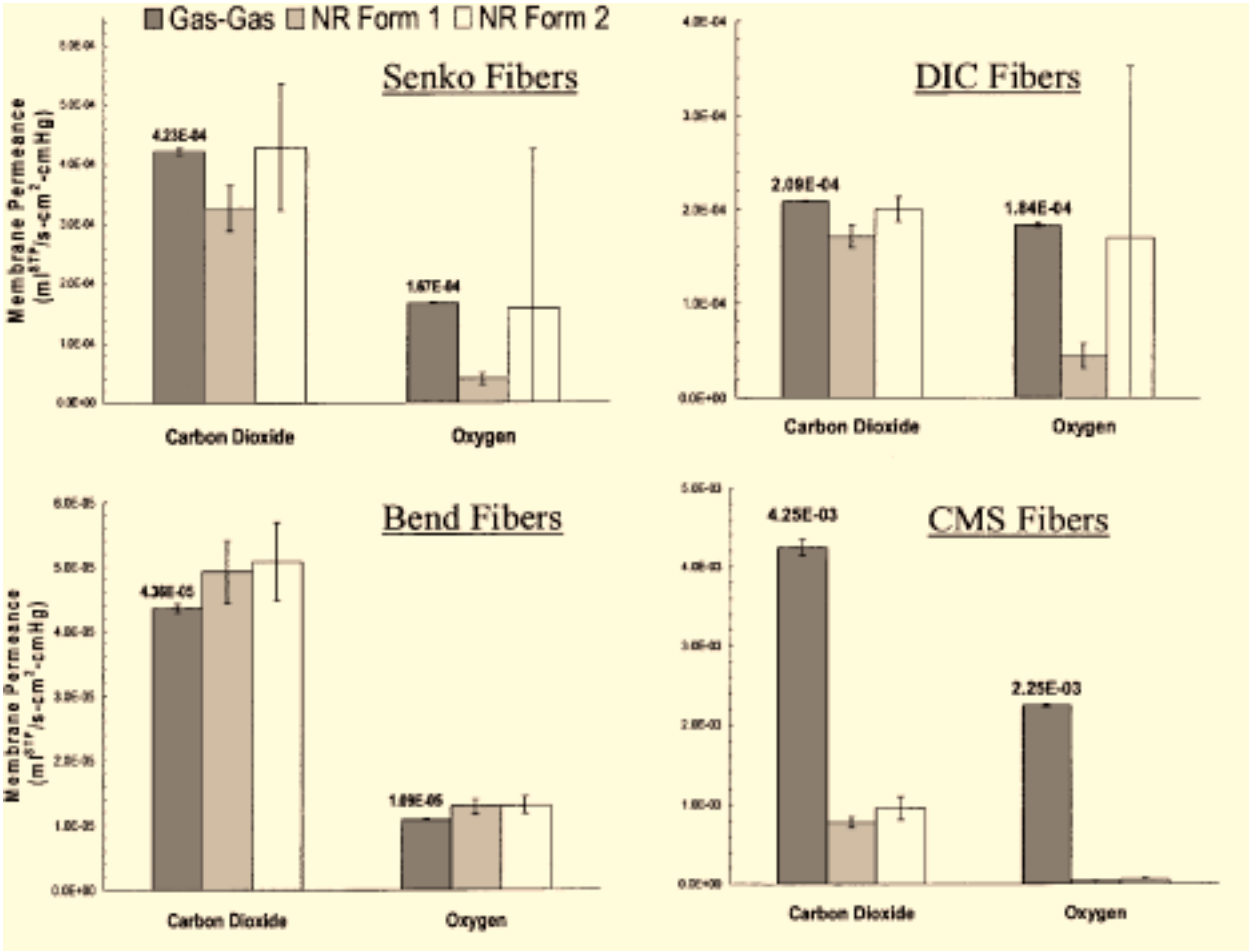

Figure 4. Membrane permeance of coated HFM estimated from gas-liquid permeance measurements using both forms of the system model, compared to measurements in a gas-gas environment.

environment is the same as its permeance in a gas-gas environment. For microporous fibers, however, this conclusion cannot be made directly from gas-liquid permeance measurements because the membrane permeance is several orders of magnitude larger than the liquid boundary layer mass-transfer coefficient at the maximal stir rate. To achieve a liquid boundary layer mass-transfer coefficient that is within an order of magnitude of the gas-gas permeance measurements of the microporous fibers, it would necessary to stir the chamber at 20,000 rpms. This puts in perspective the difficulty in eliminating boundary layer effects when measuring high permeance fibers in a gas-liquid environment, and is very likely the cause of the lower-than-expected permeance measurements of microporous fibers in a gas-liquid environment made by previous investigators. Perhaps, by combining this methodology and the techniques used by Keller and Shultis (1979) and Qi and Cussler (1985), a higher range of membrane permeance estimation might be achieved.

However, it can be shown indirectly from the gas-liquid permeance measurements that the membrane permeance of a microporous fiber in a gas-liquid environment is also the same as its permeance in a gas-gas environment. By assuming the microporous membrane permeance in a gas-liquid environment to be the same as that which was measured in the gas-gas environment, the membrane resistance will be negligible with respect to the liquid boundary layer resistance. For such a difference in resistances, the system model can be simplified to

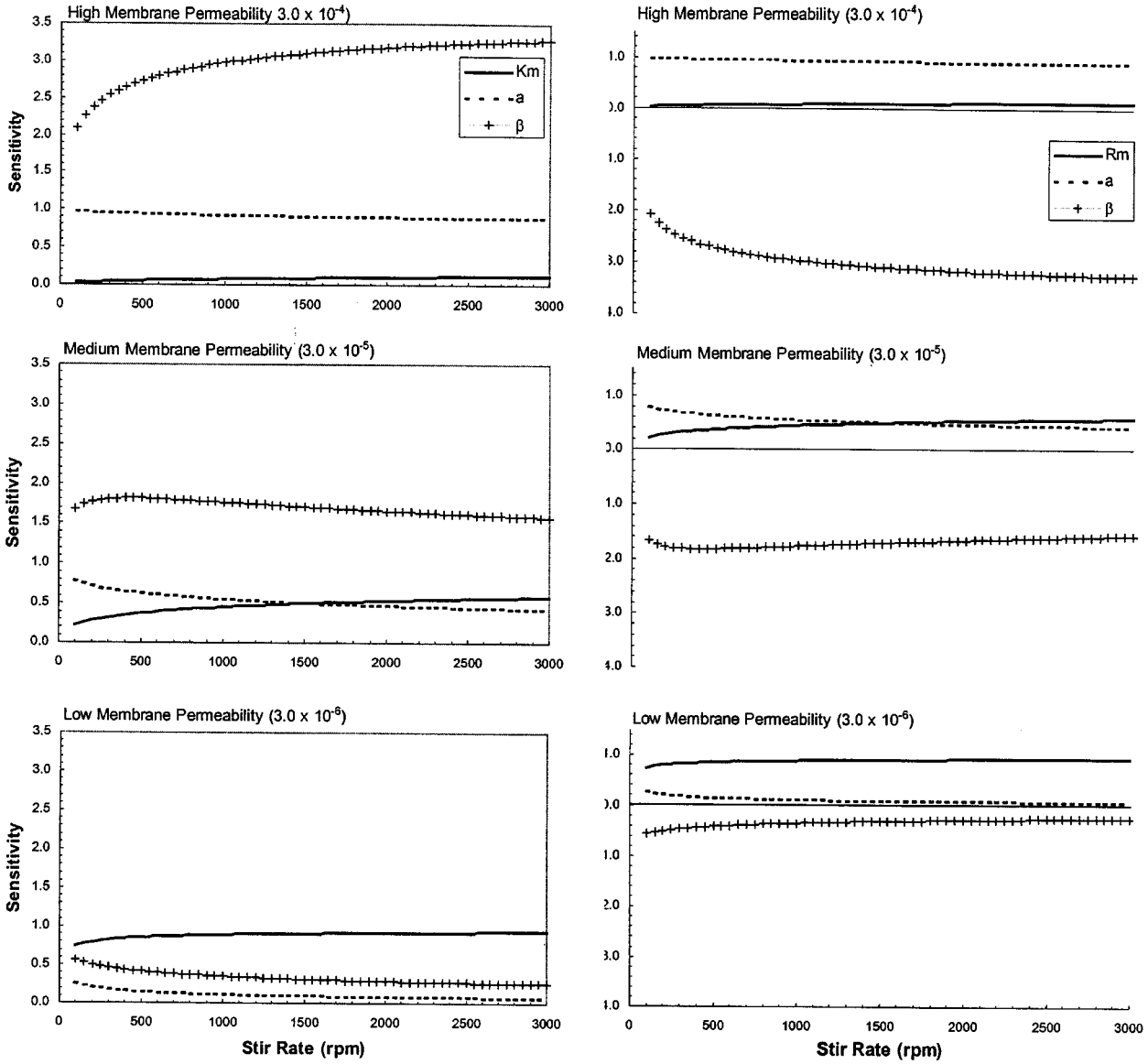

Figure 5. Normalized sensitivity coefficients as a function of stir rate based on Form 1 for the left side and Form 2 for the right.

The top plots are based on a K_m one order of magnitude greater than the maximum measured K_λ. The middle plots have a K_m equal to the maximum K_λ, while the lower plots have a K_m one order of magnitude less than the maximum K_λ. The solid lines are K_m sensitivity.

$$K = K_\lambda = \alpha \Omega^{\beta} \tag{11}$$

The parameters α and β can be easily determined with this simplified model using linear regression to the gas-liquid permeance data on a log-log plot, where β is estimated from the slope of the line fit, and α is estimated from the antilog of the intercept. The liquid boundary layer mass-transfer coefficient K_λ of the microporous Celgard X30-240 HFMs should be the same as that for the coated X30-240 fibers, and, thus, the K_λ determined directly from the log-log plots of the microporous HFM gas-liquid permeance data can be used to calculate the K_m for the coated fibers using Eq. 6. The membrane permeances calculated in this way were found to be consistent with the gas-gas measurements of the coated fibers. If in fact the permeance of the microporous membranes in a gas-liquid environment were significantly lower due to pore infiltration, than the mass-transfer coefficients estimated directly from the log-log plot of the gas-liquid permeance measurements would have been overestimated, and the coated fiber permeance calculations would have been underestimated (Lund, 2000).

Conclusions

The methodology for measuring the permeance of HFMs in a gas-liquid environment is limited by the maximum obtainable Reynolds number for the flow of liquid past the fibers in the system used. It was shown that the nonlinear regression methodology was successful in isolating membrane permeances which were as high as an order of magnitude greater than the liquid boundary layer mass-transfer coefficient at the maximum stir rate used to measure system permeance. For membrane permeances equal to or less than the maximum stir rate mass-transfer coefficient, the methodology was able to estimate membrane permeance to within 10%. For the diffusion chamber used for this research, the maximum stir rate boundary layer mass-transfer coefficients were 1.2×10^{-5} $mL^{STP}/s\cdot cm^2\cdot cm$ Hg for oxygen and 2.5×10^{-4} $mL^{STP}/s\cdot cm^2\cdot cm$ Hg for carbon dioxide. Thus, because oxygen is approximately an order of magnitude less soluble in water than carbon dioxide, the liquid boundary layer mass-transfer coefficient and, hence, the gas-liquid permeance methodology is more limited for oxygen than for carbon dioxide, as reflected in the estimation results.

Using Form 2 of the model, the methodology was successfully able to estimate oxygen permeances from gas-liquid permeance data with the DIC and Senko fibers for which the gas-gas permeances were shown to be approximately ten times greater than the maximum stir rate mass-transfer coefficient for oxygen. It was found that for the diffusion chamber data, the methodology worked much more effectively with Form 2 of the system model ($R = R_m + \gamma\Omega^{-\beta}$).

The benefits of the diffusion chamber design used for this research were that small liquid volumes could be used, new fiber samples could be quickly and inexpensively prepared, and high liquid velocities could be achieved using the impeller compared to the other potential design configurations. The primary drawback of the design was that the mass-transfer correlation of the flow pattern was unknown. However, the mass-transfer correlations determined directly from log-log plots of the system permeance measurements with high permeance microporous fibers were shown to correctly predict the permeance of coated fibers and thus were concluded to be accurate characterizations of the liquid boundary layer mass transfer for HFMs in the diffusion chamber.

The methodology for isolating membrane permeance in a gas-liquid environment from the liquid boundary layer mass-transfer coefficient is useful to evaluate the effects of special factors associated with a specific liquid (such as blood) in contact with the fiber on membrane permeance. However, it must be noted that to use this methodology requires knowledge of or the ability to measure the solubility of the test gas in the liquid of interest, since the overall system permeance is determined from the solubility, washout decay rate, liquid volume, and fiber surface area per Eq. 3. If solubility is not known, the methodology is still valuable to study the relative change in membrane permeance for a given liquid using the liquid boundary layer mass-transfer correlations determined with water.

Acknowledgments

The authors would like to thank Dr. Kenneth Lutchen for his time and expertise regarding nonlinear regression.

Literature Cited

Beck, James V., and Kenneth J. Arnold, *Parameter Estimation in Engineering and Science*, Wiley, New York, p. 379 (1977).

Brodkey, Robert S., and Harry C. Hershey, *Transport Phenomena: A Unified Approach*, McGraw-Hill, New York, pp. 182–186 (1988).

Hu, Chen-Ze, Eric K. Dolence, Shigemasa Osaki, and Clifton G. Sanders, Hydrocyclosiloxane Membrane Prepared By Plasma Polymerization Process, U.S. Patent No. 5,463,010 (1995).

Keller, K. H., and K. L. Shultis, "Oxygen Permeability in Ultrathin and Microporous Membranes during Gas-Liquid Transfer," *Trans. of Amer. Soc. of Artificial Internal Organs*, Vol. 25, 469 (1979).

Lund, L. W., W. J. Federspiel, and B. G. Hattler, "Gas Permeability of Hollow Fiber Membranes in a Gas-Liquid System," *J. Memb. Sci.*, **117**, 207 (1996).

Lund, Laura W., "Measurement of Hollow Fiber Membrane Permeance in a Gas-Liquid Environment," PhD Diss., University of Pittsburgh (2000).

Lutchen, Kenneth R., Zoltan Hantos, and Andrew C. Jackson, "Importance of Low-Frequency Impedance Data for Reliably Quantifying Parallel Inhomogeneities of Respiratory Mechanics," *IEEE Trans. on Biomed. Eng.*, **35**, 472 (Jun. 1988).

Lutchen, Kenneth R., and Andrew C. Jackson, "Reliability of Parameter Estimates From Models Applied to Respiratory Impedance Data," *J. of Appl. Physiol.*, **62**, 403 (1987).

Nemser, Stuart M., and Ian C. Roman, Perfluorodioxole Membranes, U.S. Patent No. 5,051,114 (1991).

Ohata, T., Y. Sawa, M. Takagi, T. Inoue, T. Yoshida, S. Kogaki, and H. Matsuda, "Hybrid Artificial Lung with Interleukin-10 and Endothelial Constitutive Nitric Oxide Synthase Gene-Transfected Endothelial Cells Attenuates Inflammatory Reactions Induced by Cardiopulmonary Bypass," *Circulation*, **98**, II-269 (1998).

Qi, Z., and E. L. Cussler, "Microporous Hollow Fibers for Gas Absorption: II. Mass Transfer across the Membrane," *J. of Membrane Sci.*, **23**, 333 (1985).

Yasuda, H., and C. E. Lamaze, "Transfer of Gas to Dissolved Oxygen in Water via Porous and Nonporous Polymer Membranes," *J. of Appl. Poly. Sci.*, **16**, 595 (1972).

Manuscript received Mar. 20, 2001.